



Published in final edited form as:

Proc IEEE Int Symp Biomed Imaging. 2011 June 9; 2011(March 30 2011-April 2 2011): 504–507. doi: 10.1109/ISBI.2011.5872455.

DIFFERENTIAL GEOMETRIC APPROXIMATION OF THE GRADIENT AND HESSIAN ON A TRIANGULATED MANIFOLD

Burak Erem and Dana H. Brooks

Center for Communications and Digital Signal Processing, Dept. of Electrical & Computer Engineering Northeastern University, 360 Huntington Ave., Boston, MA

Abstract

In a number of medical imaging modalities, including measurements or estimates of electrical activity on cortical or cardiac surfaces, it is often useful to estimate spatial derivatives of data on curved anatomical surfaces represented by triangulated meshes. Assuming the triangle vertices are points on a smooth manifold, we derive a method for estimating gradients and Hessians on locally 2D surfaces embedded in 3D directly in the global coordinate system. Accuracy of the method is validated through simulations on both smooth and corrugated surfaces.

Index Terms

Gradient; Laplacian; ECG; EEG

1. INTRODUCTION

Smooth manifolds embedded in Euclidean space can be useful representations of surfaces of great relevance in biomedical imaging applications. In particular, in electrocardiography (ECG) and electroencephalography (EEG), the body, heart, scalp, and cortical surfaces can all be usefully represented as manifolds when electric potentials are directly recorded by electrode arrays on those surfaces or estimated on them from remote measurements. First- and second-order spatial derivatives of these potentials are useful in a number of settings, including both the processing of recorded data and regularization of an inverse problem [1, 2, 3, 4, 5]. However, in practice, we do not have knowledge of complete manifolds, but rather a collection of measurement or estimation locations, taken to be points on a manifold, along with potential values at those locations, and we must approximate the derivatives of interest. In this setting, the manifolds are represented by this (relatively sparse) sampling of points, typically connected via a triangularization to represent the local relationships of the points on the surface. Motivated by this setting, we present here a method for approximating the gradient and Hessian of scalar functions on a discrete set of points that lie on a manifold embedded in a Euclidean space.

Previous work on estimating spatial derivatives of electrical potential on such surfaces have generally consisted of methods that approximate either the gradient or the Laplacian (the trace of the Hessian matrix). Typically the approach of these methods is to approximate the triangulated mesh locally by a surface (such as a plane [2], sphere [6, 5], or thin plate splines [7]), on which a local coordinate system is constructed. In the case of the approximated gradient, this requires an *a posteriori* set of rotations, one for each local coordinate system, to return to global coordinates. The data on the surface is approximated by a function whose derivatives are known (such as polynomial approximation [6], first- and second-order Taylor polynomials [2, 5], or analytic splines [7]) on the local coordinate system.

In the work presented here, we assume that the nodes, or vertices, of the triangulated surface, but not necessarily the planar triangles themselves, lie on a smooth manifold, and use differential geometry to obtain a natural approach to approximating the derivatives of interest. In place of an explicit parameterization of the surface, we represent the surface by the collection of normal vectors at each node. Given this surface representation, we also use a functional approximation of the data, fitting a second-order Taylor polynomial. With this approach we are able to simultaneously approximate the gradient and Hessian with a formulation entirely in global coordinates.

In this paper we describe the mathematical background, present our methods, and present simulated experimental results and discussion of the results of our method as applied both on the unit sphere and on a corrugated surface.

2. BACKGROUND

In this section we will discuss our assumptions about the manifold of interest and its relationship to the triangulated representation. We describe how the properties of derivatives on manifolds allow us to formulate a method in global coordinates. Because of our interest in electroencephelography and electrocardiology applications, our presentation here focuses on triangulated surfaces of two dimensional manifolds in \mathbb{R}^3 , although the method could be generalized to higher dimensions in a straightforward manner.

2.1. Triangulated Manifolds in \mathbb{R}^3

A triangulated surface consists of a set of nodes or points $\{x_i\}_{i=1}^K \in \mathbb{R}^3$ that are taken as vertices connected by edges to form triangles. Each triangle is identified by a triplet of node indices. In this work we assume that the nodes $\{x_i\}_{i=1}^K$ lie on the manifold, but that the edges and the planar segments defined by the triangles may not. We will refer to the set of nodes connected to a given node as its local neighbors on the surface.

2.2. Differentiation on Manifolds

Formally, our goal is to find the first and second derivatives of an analytic function $f: \mathcal{M} \rightarrow \mathbb{R}$ that maps a manifold \mathcal{M} to the scalar reals. We assume that \mathcal{M} is a 2-dimensional smooth manifold embedded in \mathbb{R}^3 . The gradient of f , denoted Df , is a vector field on the manifold \mathcal{M} and hence consists of vectors restricted to the 2-dimensional Euclidean space tangent to the manifold at any point [8]. It follows that the projection of the gradient row vector $Df(x)$ onto the vector n normal to \mathcal{M} at the point x satisfies $Df(x)n = 0$. Similarly, the quadratic form of the Hessian matrix $D^2f(x)$ with the normal vector n satisfies $n^T D^2f(x)n = 0$. Consequently, in order to find Df and D^2f we can use global coordinates to first differentiate the function f as a mapping from \mathbb{R}^3 to \mathbb{R} and then enforce the restriction to the tangent space of the manifold.

3. METHODS

3.1. Local Approximation by Second-Order Taylor Polynomial

To calculate the gradient and Hessian for a given set of nodes, we fit a second-order Taylor polynomial to each node and its local neighbors. To simplify the notation in our derivation, without loss of generality we will assume that the node of interest is at the origin and that its

local neighbors are the points $\{p_i\}_{i=1}^{K_p}$. Under this assumption, the value of the function f at a local neighbor p_i in terms of its second-order Taylor polynomial approximation is:

$$\begin{aligned}
f(p_i) &\approx f(0) + Df(0)p_i + \frac{1}{2}p_i^T D^2 f(0)p_i \\
&= f(0) + Df(0)p_i + \frac{1}{2}\text{tr}(p_i^T D^2 f(0)p_i) \\
&= f(0) + Df(0)p_i + \frac{1}{2}\text{tr}(p_i p_i^T D^2 f(0)) \\
&= f(0) + Df(0)p_i + \frac{1}{2}\text{vec}(D^2 f(0))^T \text{vec}(p_i p_i^T)
\end{aligned} \tag{1}$$

where the $\text{vec}(\cdot)$ operator vectorizes a matrix by vertically appending its columns in order. This is extended to all the neighbors of a node by formulating the linear matrix equation:

$$\begin{bmatrix} f(p_1) - f(0) & \cdots & f(p_{K_p}) - f(0) \end{bmatrix} = \begin{bmatrix} Df(0) & \text{vec}(D^2 f(0))^T \end{bmatrix} \times \begin{bmatrix} p_1 & \cdots & p_{K_p} \\ \frac{1}{2}\text{vec}(p_1 p_1^T) & \cdots & \frac{1}{2}\text{vec}(p_{K_p} p_{K_p}^T) \end{bmatrix} \tag{2}$$

We find $Df(0)$ and $D^2 f(0)$ such that they are restricted to the tangent space. We also force $D^2 f(0)$ to be symmetric by consolidating variables when they are identical. Given both the symmetry and the constraints on the derivatives to lie in the tangent space, in \mathbb{R}^3 there are 2 degrees of freedom for the gradient and 3 for the Hessian. Thus, when $K_p < 5$, (2) is guaranteed to be underdetermined. In the underdetermined case, we find the minimum norm solution that satisfies (2), otherwise we find the least squares solution.

3.2. Gradients and Hessians by Matrix Multiplication

We next introduce a computationally simpler approach to the calculation just described. A key observation is that, given a function on a predefined set of nodes $\{x_i\}_{i=1}^K$, the method described solves for Df and $D^2 f$ at each node using only linear operations. Suppose that we define a vector $F \in \mathbb{R}^K$ of function values of f at the nodes $\{x_i\}_{i=1}^K$:

$$F = \begin{bmatrix} f(x_1) & \cdots & f(x_K) \end{bmatrix}^T \tag{3}$$

and a collection of the consolidated forms of their respective gradients and Hessians:

$$f_{\text{gh}}(x_i) = \begin{bmatrix} Df(x_i) & \text{vec}(D^2 f(x_i))^T \end{bmatrix} \tag{4}$$

$$F_{\text{gh}} = \begin{bmatrix} f_{\text{gh}}(x_1) & \cdots & f_{\text{gh}}(x_K) \end{bmatrix}^T. \tag{5}$$

Then the linearity of the method means that it can be simplified to multiplication by a matrix D :

$$F_{\text{gh}} = DF \tag{6}$$

We extract the matrix D by applying the gradient and Hessian method at every node for the canonical basis functions $\{e_i\}_{i=1}^K \in \mathbb{R}^K$. Thus column i of the matrix D is the result of the gradient and Hessian method applied to the vector with element i equal to 1 and zeros elsewhere. Furthermore, one could isolate a matrix for calculation of just the gradient, G , or just the Hessian, H , by keeping only the relevant rows from the matrix D .

4. EXPERIMENTAL RESULTS

To evaluate our approach under controlled conditions, we synthesized two tractable surfaces, a triangulated unit sphere and a corrugated surface, on which we generated example functions. In both cases we compared results using the known function to supply the “data”, so that we had analytical derivatives available for comparison to the estimates. For these experiments we supplied our method with the true normal vectors at each node in order to facilitate a fair comparison to the analytical results.

4.1. Triangulated Unit Sphere

For our first experiment, we generated a unit radius triangulated sphere populated by 642 nodes and 1280 triangles. On this set of nodes, we generated a quadratic function of the form $f(v) = v^T A v + b^T v$, where $v = [x, y, z]^T$, on which to evaluate our method. We calculated the gradient and the Hessian jointly as described above. Statistics of the results are shown in the first row of Table 1. We report the norm of the analytical gradients, correlation between the analytical and approximated gradients, and error norm of the difference normalized by the norm of the true gradients. We also calculated the Laplacian using Huiskamp’s method [2], which is a widely used approach in a number of subfields of computational electrocardiography. We compared the Huiskamp method results to the Laplacian values extracted from our Hessian, and found that they were comparable in terms of accuracy. We note that finding gradients using a method based on an extension of the Huiskamp method is somewhat problematic because of the need to go from local to global coordinate systems, whereas with the approach presented here we get the gradients, Laplacian, and indeed the entire Hessian, all at once.

4.2. Corrugated Surface

For this pair of experiments, we created a simple model of a surface with ridges and valleys, inspired by the sulci and gyri of the cortical surface. We started with a rectangular region in the x-y plane which was transformed by a diffeomorphism to form a sinusoidal corrugated surface. The original planar surface was triangulated such that it had 1600 nodes and 3080 triangles. The diffeomorphism $(x, y) \rightarrow (x, y, \sin(4\pi x))$ was used as the transformation. We defined a radial logistic function of the form $f(x, y, z) = (1 + \exp(-\beta(x, y, z)))^{-1}$ to simulate the measurements made on the surface. We simulated measured or estimated data in two ways: in the first $\beta(x, y, z)$ was a quadratic function that depended only on x and y, while it depended on all of its inputs in the second. The top row of the left column of Figure 1 shows the first case, where we have a cylindrical shape that intersects the surface, whereas the second case is in the bottom row of the left column, and shows a three-dimensional ellipsoidal shape that intersects the surface. On the right side of Figure 1, we show a map of the relative error of the gradient approximated at each node after “unwarping” the surface back to the plane.

5. DISCUSSION

As our results show, our method accurately approximated the gradient on a triangulated manifold surface. The Laplacian extracted from our approximation of the Hessian compared well with the Laplacian estimator in [2]. The strength of the proposed method is that it makes use of the assumption that the measurement locations lie on a smooth manifold without approximating the whole surface. This results in a formulation that works directly in global coordinates and whose linearity allows us to computationally simplify the method to a set of matrix-vector multiplications. A potential disadvantage is that, in practice, our method may be supplied poorly approximated normal vectors that will cause a decrease in the accuracy of its results. We note that this weakness is shared by methods that functionally

approximate the surface via planar triangles or other piecewise surfaces as well. Another shared limitation is that we only fit a quadratic in our local approximation of the data and hence would expect a less accurate fit to a higher order function. Of course both limitations are also affected by the measurement density compared to the curvature of the surface, as would be true for any general approximation method. This can be seen in both cases in the right column of Figure 1, where the largest relative errors occur at nodes along the edges of the mesh which tend to have less neighbors.

As we stated in the introduction, we envision a number of applications for this method in the field of biomedical imaging and particularly ECG and EEG. For example, in the processing of recorded data on a surface mesh, a common use of derivatives is for interpolation of known data to new nodes by minimization of the Laplacians [1]. In the context of inverse problems, both the gradient and Laplacian have frequently been used to regularize the inverse problems of both modalities (e.g. Tikhonov regularization) by bounding the derivatives of solutions on the surface of interest [2, 3, 4, 5]. Identification of nodes on a surface mesh with high gradient magnitude, along with the gradient direction, can be used for edge detection or detection of spatio-temporal phenomena such as local bursts of activity on the cortex or cardiac wavefront arrival on the heart [9]. As a specific example, we have applied the method in the context of computational cardiology to find the arrival time of cardiac wavefronts on the epicardial surface of the heart. We combined this method of estimating the surface gradient with a temporal derivative by looking for the extrema of an appropriate combination of the two estimators. Results have been quite promising compared to standard methods but space precludes a detailed presentation of the comparison here. More detail on this application will be presented during the conference.

Acknowledgments

The work of the authors was supported in part by the NIH/NCRR BTRC Center for Integrative Biomedical Computing (CIBC), 2 P41 RR 012553 - 12.

References

1. Oostendorp TF, van Oosterom A, Huiskamp G. Interpolation on a triangulated 3D surface. *J Comput Phys.* 1989; 80(2):331–343.
2. Huiskamp G. Difference formulas for the surface Laplacian on a triangulated surface. *J Comput Phys.* 1991; 95(2):477–496.
3. Baillet S, Mosher JC, Leahy RM. Electromagnetic brain mapping. *Signal Proc Mag.* 2002; 18(6): 14–30.
4. Kaipio, JP.; Somersalo, E. *Statistical and computational inverse problems.* Springer Science+ Business Media, Inc; 2005.
5. Alecu, TL.; Voloshynovskiy, S.; Pun, T. ISBI. 2004. EEG cortical imaging: a vector field approach for Laplacian denoising and missing data estimation; p. 1335-1338.
6. Barnhill RE, Ou HS. Surfaces defined on surfaces. *Comput Aided Geom D.* 1990; 7(1–4):323–336.
7. Babiloni F, Babiloni C, Carducci F, Fattorini L, Onorati P, Urbano A. Spline Laplacian estimate of EEG potentials over a realistic magnetic resonance-constructed scalp surface model. *Electroen Clin Neuro.* 1996; 98(4):363–373.
8. Tu, LW. *Introduction to manifolds.* Springer Verlag; 2007.
9. Punske BB, Ni Q, Lux RL, MacLeod RS, Ershler PR, Dustman TJ, Allison MJ, Taccardi B. Spatial methods of epicardial activation time determination in normal hearts. *Ann Biomed Eng.* 2003; 31(7):781–792. [PubMed: 12971611]

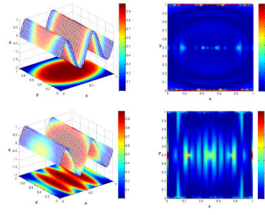


Fig. 1. (*left*) Functions displayed on corrugated surface mesh and its projection onto the x-y plane and (*right*) relative error of gradient approximations at simulated corrugated surface mesh nodes projected onto the x-y plane. Results for (*top*) cylindrical and (*bottom*) ellipsoidal radial logistic functions.

Table 1

Performance of approximated vs analytical gradients

Experiment	Grad. Norm	Correlation	Rel. Error
Unit Sphere	80.1073	1.0000	0.0085
Corrug: Cyl.	102.0496	0.9996	0.0309
Corrug: Elli.	67.3724	0.9978	0.0670